

Radiosonde Refractivity Data Analysis Using Neural Network Techniques

Ibrahim A. Altawil, Mohammad H. Bataineh and Deifallah A. Dajeh
 Hjjwi Faculty for Engineering Techology Yarmouk University, Irbid, Jordan

Abstract: This study discusses the mapping of an important climatic parameter which is crucial in statistical path loss procedures adopted by the International Telecommunications Union (ITU). This parameter is the probability that the refractivity in the lowest 100 m of the atmosphere is less than -100 N-units/km (denoted by β_0). This parameter is available where radiosound station collect their measurements. The interest is to be able to give a value to this indicative parameter" ideally 'everywhere in the world. The available 'row' data are contour plotted on a world map. Improvements on these maps is suggested by gridding the world into 'small' squares and evaluating the value at each corner of the square by interpolating with adjacent values. Artificial neural networks is used also as a processing technique to approximate the function representative of the β_0 data so as to develop models by which the values of β_0 could be estimated in locations where data is not available. The technique has been used successfully to estimate β_0 values in the North Western quarter of the hemisphere taken, for example. The results shown in this paper are based on data collected from about 4400 locations throughout the world for the years 1983-1992. The paper compares and contrasts the neural network approach to a suggested estimation methodology and it is shown that good agreement is obtained.

Key words: Radiosonde redractivity, data analysis, nrural network

INTRODUCTION

The planning of radio services requires a good knowledge of the propagation characteristics of the physical areas of interest. Such information is required, not only to ensure that an adequate service will be provided, but also to help assess the potential of interference between stations working in the same band, or in a worse case, sharing the same frequency. Under some climatic conditions it is possible for a radiowave to propagate over distances well beyond their radio horizon limit, causing interference between distant base stations.

A significant parameter used extensively by radio meteorologists which takes account of climatic variations (such as temperature, pressure and humidity) is the radio refractivity^[1]. A statistical study of the gradient of this parameter in the lowest 100 m is a particular importance in tropospheric radiowave propagation. If it happens that this gradient is less than-100 N-units/km "ducting" conditions form^[2]. The first study of this type was carried out in the 1960s^[3]. This study involved 112 radiosonde stations and covered a time span of five years (using figures for four months from each year). The results of this study still form the basis of the recommended prediction procedures for line-of-sight paths^[4] and for interference between terrestrial stations^[5] made by the International Telecommunication Union (ITU). A more extensive study of refractivity statistics, based on five years of data (including all calendar

months) obtained from over 900 stations, was carried out in the late 1970s^[6] for the United States Department of Defence, (DoD).

The study described in this paper is based on more recent and more extensive radiosonde data obtained from the National Centre for Atmospheric Research (NCAR), USA. This data is used to investigate and map physically-based refractivity parameters representative of the troposphere during anomalous propagation conditions. Also, because the data is collected at specific locations, a method to predict data in unmeasured locations is vital in any planning procedure. Neural network and another proposed technique have been used to estimate β_0 in locations where it is not measured.

Data mapping: For each station, the percentage of time that the gradient of the refractivity in the lowest 100 m is less than-100 N-units/km has been obtained. Whilst the results in the above form are suitable for examining one particular location, it is difficult to compare differences between various stations in detail. Therefore, it seems appropriate to map the values obtained on a geographical basis, so that variations according to locations can be assessed. Figure 1 shows contours, superimposed on a world map, for values of β_0 . These have been colour coded according to the legend shown under the map. Although there are not as many stations in the southern hemisphere as in the northern hemisphere, the map shows the expected trend of an increase from the continental

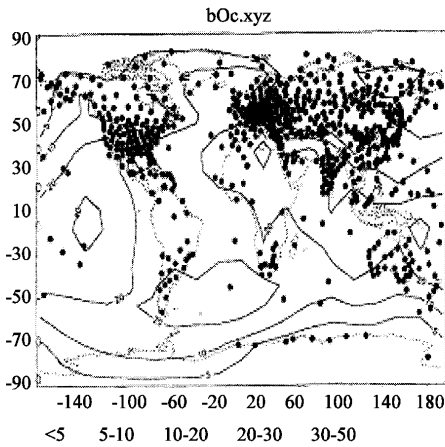


Fig. 1: contour of β_0

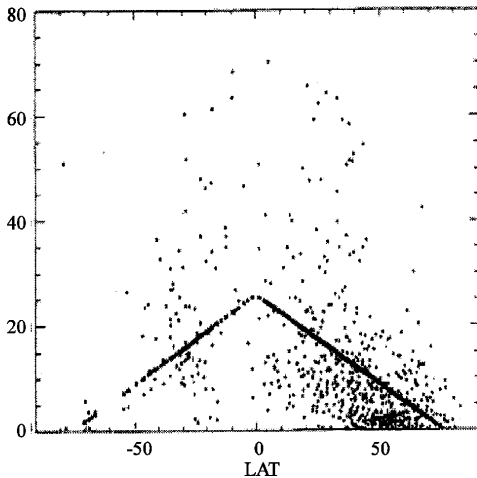


Fig. 2: β_0 values with the best fit

climate in the north eastern Europe to the Mediterranean climate in the south. As the figure suggests there is an apparent variation in ducting parameters with latitude. Therefore, we can remove this ‘strong trend’ by fitting the values to the best curve under a least mean square error criterion. From this the differences between the actual values and fitted curve (i.e., the residuals) can be presented on a world map, which is shown in Fig. 2. The β_0 -map is of particular importance^[4-8] and therefore the parameters affecting its values are to be investigated further by applying this approach.

The β_0 values plotted against latitude, are shown, with the best fit-curve, in Fig. 2. The curve used here is of the form:

$$f = 25.7 - 0.4|Lat| \tag{1}$$

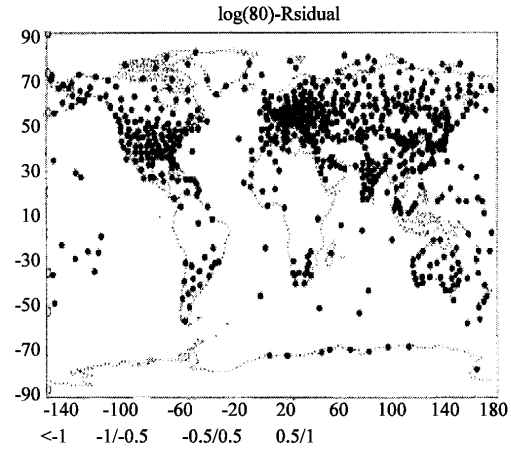


Fig. 3: Residual map of β_0

The residuals, i.e., the differences between the actual β_0 values and the fitted curve, are plotted on a world map as shown in Fig. 3. This figure gives insight of regions of high incident of ducting and the effect of coastal areas emerge clearly; represented here by ‘positive’ colour dots.

Designed estimation technique: The contour map shown in Fig. 1 has been plotted after producing a regular ‘grid’ of obtained data from the original raw measurements obtained at radiosonde stations locations. The production of the uniform grid requires an interpolation at ‘grid’ or ‘node’ points. Here an optimal Kriging algorithm has been used to generate these points^[9]. The Kriging algorithm used in various geologic and geographic map-making^[10] and in ionospheric characteristic mapping^[11,12].

The ‘matrix’ of the resulting grid has then been used to estimate the values at any location. A requirement of an estimation function is to give the value estimated by the Kriging algorithm if it happens that one would like to check the validity of the function. In addition to that the value at the centre of the grid should be the average of the node values. This initiative requirement may be translated to the following formula:

$$f = \frac{\sum_{i=1}^4 w_i v_i}{\sum_{i=1}^4 w_i} \tag{2}$$

The values at the four corners are give the symbol v . Here, w ’s weighting the values in accordance to the location in the grid. As one approaches any node more weight should be given to that node. Therefore, w ’s are related to the fares or proximately from the node points, i.e., to distances from the corners and they are given by

$$\begin{aligned}
 w_1 &= d_2 d_3 d_4 \\
 w_2 &= d_1 d_3 d_4 \\
 w_3 &= d_1 d_2 d_4 \\
 w_4 &= d_1 d_2 d_3
 \end{aligned}
 \tag{3}$$

This estimation function has been used to find the values of β_0 for various radio paths in Europe and the values could be used to find out the effect of the climate on line-of-sight propagation.

Artificial neural networks: Neural networks offer an excellent approach for computing inspired by the brain's behaviour. The elements (neurones models) are thought to mimic the basic behaviour of real human neurones. Different forms of inter-connection of neurones will produce different neural network strategies such as feedforward and recurrent networks^[13]. The strength of the neural networks approach is its ability to generalise from the training examples to the entire domain and also its ability to accommodate noise and poor data. This offers new opportunities for the approximation and identification of nonlinear system^[14].

Brief description of multilayer feed forward neural networks: Neural network is employed in this respect because of its powerful learning and memorising characteristics. In this application a multilayer feedforward net work as shown in the Fig. 4 is used. This type of neural network has an input layer, one output layer and any number of hidden layers in between. The net input neurone j is therefore described by

$$net_j = \sum w_{ji} o_i + \theta_j$$

where o_i is the output of neurone in the previous layer, θ_j is the threshold of neurone j in the present layer and w_{ji} is the weight of connection from neurone i to neurone j . The output of neurone j is computed by passing the net_j through a nonlinear function. The nonlinear activation function used here is a sigmoidal function and the output of neurone j is as follows:

$$o_j = \frac{1}{(1 + \exp(-net_j))}$$

Usually in feedforward neural networks all the nodes in hidden and output layer have the same structure as shown in the Fig. 5. The learning ability of this work is originated from the modification of weights among neurones during training stage. The algorithm for modification of weights in multilayer networks was proposed by Kroenke 2002^[15].

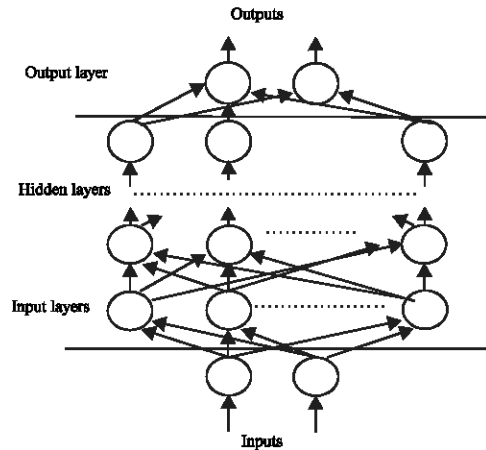


Fig. 4: Multilayer feedforward net work

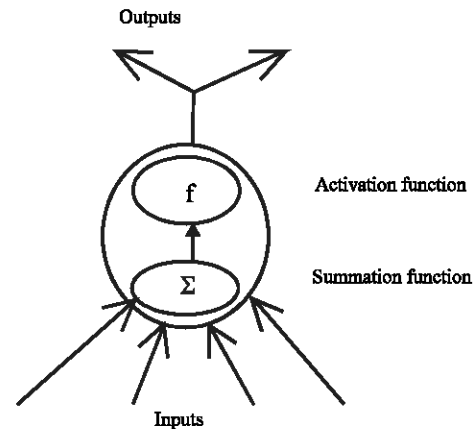


Fig. 5: Multilayer feedforward net work with activation and summation function

In the learning stage. The input pattern are now the location of β_0 in longitude and latitude. The back propagation algorithm adjusts the weight so that the error E can be reduced as

$$E = \frac{1}{2} \sum (t_{pk} - o_{pk})^2$$

where t_{pk} and o_{pk} are the desired target and output of neural network for pattern respectively. The weights are update in the gradient descent direction of E , i.e.,

$$\Delta w_{ji} = -\eta \frac{\partial E}{\partial w_{ji}}$$

where Δw_{ji} is the amount of change for the weight component w_{ji} and the positive constant η is the learning rate of the neural network. The larger η is the faster the change in the weights but it may lead to in the

weight space. For a feed forward neural network with sigmoidal activation function, the evaluation of are

$$\frac{\partial E}{\partial w_{ji}}$$

$$\Delta w_{ji} = \eta \delta_{pj} o_{pi}$$

with

$$\delta_{pi} = (t_{pk} - o_{pk}) o_{pj} (1 - o_{pj})$$

for output layer

$$\delta_{pj} = o_{pj} (1 - o_{pj}) \sum \delta_{pj} w_{kj}$$

oscillation

For hidden layer. In this application, a large number of training patterns were used to generate a reliable input data. One of the modification algorithm suggested by Rumelhart is a momentum term is given by

$$\Delta w_{ji} (n+1) = \eta \delta_{pi} o_{pi} + \alpha \Delta w_{ji} (n)$$

where N labels the iteration in the learning process and α is a momentum constant. The momentum constant determine the effect of post weight changes on the current direction of movement in weight space and fasten the learning process.

The study described here, aims to apply neural network techniques to build a model of the radio climatic parameter β_0 . This can be generalised the train data to the entire domain and hence produce an integrate model of the data. The nonlinear model can then be used to predict values of β_0 in locations where data is not actually measured. Note in particular that β_0 is a nonlinear function with respect to longitude and latitude as depicted in Fig.6.

The neural network chosen was of a feedforward type, using backpropagation momentum algorithm for weight updating. This multilayerd networks have two inputs nodes (longitude, latitude) and 35 hidden nodes and one output node β_0 . The nonlinear transfer function of the nodes was chosen to be a sigmoide function. The training parameters in the backpropagation algorithm, i.e., the learning rate and the momentum term, were appropriately selected, the learning rate being 0.1 and the momentum term 0.95. The network training was stopped when the error reached less than 0.05.

The neural network training results of this experiment are shown in Fig. 7. Here the approximated data generated by the neural network model is shown in dashed lines and the real data shown by continuous lines.

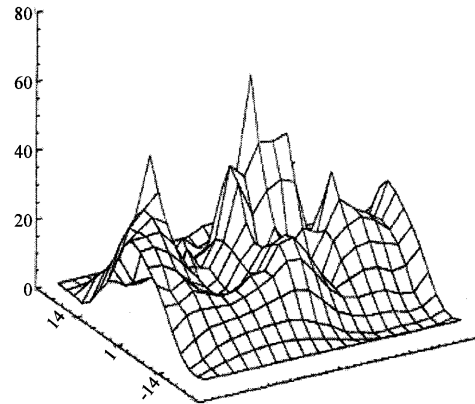


Fig. 6: A 3D of β_0 values versus longitude and latitude

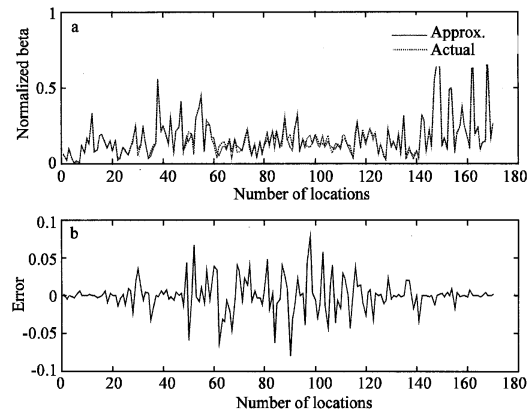


Fig. 7 (a): Approximated normalised β_0 and real β_0 measurements (b) The difference between the Approximated and actual measurements

RESULTS

The neural network was tested by applying input patterns representing locations where actual β_0 is not available and compared with values obtained using the estimation technique mentioned earlier. A few comparative examples are shown in Table 1.

The differences between the two methods is not totally surprising since the results of the first estimation method are derived from the data in the grid, while the results using neural network were generated using row data. The second, however, is straightforward and reliable and illustrate the opportunity to utilise such technique in this field.

Table 1: Results using two independent methods

Longitude	Latitude	Estimation function	Neural network
-157.7	71.3	4.804415	3.163421
-153.5	57.7	8.055639	6.566674
-144.6	70.2	4.565425	4.735425
-140.6	59.5	10.48876	8.053409
-136	60.7	8.26902	7.343859

CONCLUSION

Two estimation techniques have been presented in this study. The first is based on the application of an estimation equation, while the second based on emerging neural network techniques. The neural network techniques have been shown to be an attractive approach to estimating such nonlinear data. Also, the study demonstrates the results generated by neural network are close to the expected range when compared to other conventional techniques. It is hoped to take the analysis presented in this study further by using the data grids to train the network in order to improve its validity and to investigate other climatic parameters which are of interest to the ITU.

REFERENCES

1. Bye, G.D., 1989. Average radio refractive index lapse rate of the lower troposphere for locations in NW Europe, IEE Conference Pub. No. 301, pp: 229-223.
2. Helvey, R.A., 1983. Radiosonde errors and spurious surface-based ducts, IEE Proceedings, Part F, No. 7, pp: 643-648.
3. Cahoon, B.A., C.A. Samson and G.D. Thayer, 1996. A word atlas of atmospheric radio refractivity, ESSA Monograph 1.
4. ITU-R Recommendation 530-4, 1992. Propagation data and prediction methods required for the design of terrestrial line-of-sight systems, 1992-CCIR Recommendations, RPN series, Propagation in non-ionised media, Geneva.
5. ITU-R Recommendation 452-5, 1992. Prediction procedure for the elevation of microwave interference between stations on the surface of the earth at frequencies above about 0.7 GHz, 1992-CCIR Recommendations, RPN series, Propagation in non-ionised media, Geneva.
6. Ortenburger, L.N., 1977. Radiosonde data analysis II", GTE/Sylvania Incorporated.
7. Craig, K.H. and T.G. Hayton, 1994. Climatic mapping of refractivity parameters from radiosonde data, AGARD, pp: 43/1-43/11.
8. Bashir, S.O., 1989. Three years statistics of refractive index gradient and effective earth radius factor for the state of Bahrain, IEE Conf. Pub. No. 301, pp: 220-223.
9. Davies, J.C., 1986. Statistics and data analysis in geology, John Wiley.
10. Oliver, M.A. and R. Webster, 1990. Kriging: A Method of Interpolation for Geographical Information Systems. Int. J. Geog. Inf. Syst., pp: 313-332.
11. Samardjiev, T., P.A. Bradley, L.J.R. Cander and M.I. Dick, 1993. Ionospheric mapping by computer contouring technique, Electronic Lett., pp: 1794-1795.
12. Terje Tjelta, Norwegian Telecom, Private Communication.
13. Fu. LiMin, 1994. Neural Networks in Computer Intelligence, Co-published by the MIT Press and McGraw-Hill, Inc.
14. Yaacob, R., 2002. Nagarajan, Ali Chekima (Eds.), Proceedings of the International Conference on Artificial Intelligence in Engineering and Technology. Kota Kinabalu, Sabah, Malaysia, pp: 458-463.
15. Kroenke, D.M., 1997. Database Processing: Fundamentals, Design and Implementation (6th Ed). Prentice Hall; USA.